Interactions between self-assembled polyelectrolyte shells and tumor cells

Hua Ai,[1] John J. Pink,[2] Xintao Shuai,[1] David A. Boothman,[2] Jinming Gao[1]
[1]*Department of Biomedical Engineering, Case Western Reserve University, 10900 Euclid Avenue, Cleveland, Ohio 44106*
[2]*Department of Radiation Oncology, Case Comprehensive Cancer Center, Case Western Reserve University, Cleveland, Ohio 44106*

Received 23 August 2004; revised 22 November 2004; accepted 23 November 2004
Published online 1 April 2005 in Wiley InterScience (www.interscience.wiley.com). DOI: 10.1002/jbm.a.30289

Abstract: Layer-by-layer self-assembled polyelectrolyte shells are a new class of micro/nanocapsules with unique physicochemical properties for potential applications in drug/gene delivery. The objective of this study was to investigate the interactions of polyelectrolyte shells (~1 μm in diameter) with MCF-7 breast cancer cells and identify key parameters that affect such interactions. Tailoring of surface properties of polyelectrolyte shells was achieved by choosing different outermost layer materials, including cationic polymers, anionic polymers, and lipid bilayers. Different surface compositions led to a wide range of electrostatic potentials from −46 to +47 mV in phophate-buffered saline buffer. Confocal microscopy studies showed that the polyelectrolyte shells were internalized into the cell cytoplasm, but not into the nuclei. Correlation of cell uptake with shell surface compositions was complicated by the adsorption of serum proteins on the surface of polyelectrolyte shells, particularly polycation-coated shells. To prevent protein adsorption, poly(ethylene glycol) (PEG) grafted poly(ethyleneimine) (PEI) copolymers (1:1, 1:5, 1:10 graft ratios) were synthesized and introduced on the shell surface. Shells coated with PEI-PEG copolymers effectively reduced protein adsorption whereas PEI-PEG copolymers with lower graft ratios achieved higher cell uptake efficiency after 24 h of incubation with MCF-7 cells. © 2005 Wiley Periodicals, Inc. J Biomed Mater Res 73A: 303–312, 2005

Key words: layer-by-layer self-assembly; polyelectrolyte shells; poly(ethyleneimine) (PEI)-poly(ethylene glycol) (PEG); shell-cell interactions

INTRODUCTION

Electrostatic layer-by-layer (LbL) self-assembly provides a convenient and versatile method to build micro/nanostructures on two- or three-dimensional substrates at the molecular level.[1–3] Hollow polyelectrolyte shells are one of the most important and unique structures developed based on this technique.[4] Construction of LbL shells involves consecutive polyelectrolyte adsorption on a colloid-template followed by decomposition of the template core. Different materials, including linear polyelectrolytes (synthetic and natural), lipids, proteins, and inorganic nanoparticles can be used in nanoassembly processes. Several advantages of polyelectrolyte shells have been noted. First, the shell membrane can be predesigned with the definitive knowledge of its molecular composition. Second, membrane thickness can be controllable by varying the number of coated layers. Third, shells can shift from an "open" state to a "closed" state by changes in environmental conditions, such as temperature,[5] pH,[6,7] or presence of organic solvents.[8] Because shell permeability can be varied using the aforementioned parameters, drugs or fluorescent dyes can be loaded into shells in an open condition and encapsulated in a closed state. Finally, the surface properties of LbL shells can be controlled by adsorption of chosen nanomaterials on the outermost layer of the shells.

Drugs,[9] enzymes,[6,7] DNA,[10] or dyes[11,12] have been loaded into shells through different loading methods. Bioavailability and functionality of loaded materials are successfully preserved in biological buffers. Ultimately, the effectiveness of these delivery systems relies on many factors, including their interactions with cells, biocompatibility, and stability in physiological environment. This study focuses on the interactions of polyelectrolyte shells with breast cancer cells. Among various physical and chemical properties, surface charge and composition are among the most important factors that affect the outcome of particle in-

Correspondence to: J. Gao; e-mail: jinming.gao@case.edu
Contract grant sponsor: National Institutes of Health; contract grant numbers: R01 CA90696, R01 CA102792

teractions with cells.[13–15] In this study, hollow polyelectrolyte shells with different outermost layers were produced to examine their effects on cell uptake using human MCF-7 breast cancer cells. The outermost layer consisted of charged polymers, proteins, or lipid bilayers that represent a wide range of surface charges and compositions. MCF-7 cells were chosen to study their interactions with LbL shells because novel drug delivery methods in the treatment of breast cancers are desperately needed and could dramatically increase the therapeutic efficacy of various chemotherapeutic agents. Cell uptake was examined by flow cytometry and confocal laser scanning microscopy (CLSM). Results from this study provide a fundamental understanding of the dependence of cell uptake on the shell surface properties. The information presented will be helpful for the future development of these novel capsules for potential applications in drug/gene delivery.

MATERIALS AND METHODS

Materials

Cationic polymers used in this study include poly(dimethyldiallyl ammonium chloride) [PDDA, molecular weight (MW) 200 kD, Aldrich], poly(ethyleneimine) (PEI, MW 25 kD, Aldrich; MW 1.2 kD, Polysciences, Inc.), poly(allylamine) hydrochloride (PAH, MW 10 kD, Aldrich), and poly-L-lysine (PLL, MW 30 kD, Sigma). Negatively charged materials include bovine albumin (MW 66 kD, Sigma), gelatin (MW 50–100 kD, Sigma), and poly(styrenesulfonate) (PSS, MW 70 KD, Aldrich). 1,2-Dipalmitoyl-*sn*-glycero-3-phosphocholine (DPPC) and 1,2-dipalmitoyl-*sn*-glycero-3-phosphate (DPPA) (Avanti Polar Lipids, Inc.) were used to form negatively charged liposomes. Copolymers PEI (25 kD)–poly(ethylene glycol) (5 kD) (PEI-PEG) (1:1, 1:5, and 1:10) were synthesized and used for coating the outermost layer of LbL shells. Negatively charged 50-nm Fluoresbrite® YG Carboxylate nanoparticles (Polysciences) were used as a fluorescent label in the polymer multilayers for the polyelectrolyte shells. Weakly crosslinked melamine formaldehyde (MF) particles (0.9 μm in diameter, Microparticles GmbH, Germany) were used as templates for self-assembly.

Syntheses of PEI-PEG graft copolymers

Monomethoxy PEG (mPEG) was first activated by esterification with maleic anhydride as reported by Shuai et al.,[16] and then conjugated to PEI by amidation. Briefly, PEI and the activated mPEG were added to a flask equipped with a magnetic stirring bar. The reaction flask was immersed in a 50°C oil bath, and then high vacuum was applied. Amidation progress was monitored using Fourier transform infrared spectroscopy. When the carbonyl group from the carboxylic acid was no longer detectable, the reaction was stopped, and the product was dissolved in methanol, precipitated in diethyl ether, and then vacuum dried. The grafting ratio of the purified copolymer was calculated from the integral values of characteristic peaks of PEG (e.g., CH_3O— at ~3.38 ppm) and PEI (—CH_2CH_2— at ~2.65 ppm) in the ^1H NMR spectrum. Controlling the stoichiometry of PEG over PEI in the reaction led to PEI-PEG copolymers with molar grafting ratios ranging from 1:1, 1:5 to 1:10.

Self-assembly of polyelectrolyte shells

All polymer and protein solutions were prepared at a concentration of 2 mg/mL in phosphate-buffered saline (PBS, pH 7.4). Gelatin and PDDA were used as a pair of oppositely charged polymers to build the initial layers on MF particle templates before the outermost layer was introduced. The shell fabrication procedure is illustrated in Figure 1. First, MF microparticles were incubated in a gelatin solution for 40 min at room temperature. Centrifugation at 4000 rpm for 5 min was used to remove free polymers in solution. The particle pellet was resuspended in deionized water and washed three times by centrifugation. A second layer of PDDA was introduced following a similar coating process as described above. In total, five bilayers of gelatin and PDDA were assembled on templates. Then another bilayer of Fluoresbrite® YG Carboxylate nanoparticles (50 nm in diameter, negatively charged) and PDDA were introduced. After LbL self-assembly, the coated particles were exposed in pH 1.2 HCl solution for 2 min to decompose the MF core. Hollow shells were obtained after washing with deionized water. In general, the common composition for all shells was $(Gelatin/PDDA)_5$ + (YG-nanoparticle/PDDA), and further layers were added to achieve different surface charge and compositions.

To obtain a negative surface coating, PSS or albumin was directly adsorbed as a final outermost layer. To obtain a positively charged layer, a coating of negatively charged PSS layer was first introduced and then other cationic polymers (e.g., PEI or PLL) were adsorbed. PEI-PEG copolymers with different graft ratios were also assembled on a PSS layer. Liposomes (100 nm, 90% DPPC and 10% DPPA) were fabricated by mechanical extrusion. Final negatively charged lipid bilayers were assembled on hollow polymer shells using an established protocol.[17] Polyelectrolyte shells were stored in Millipore H_2O (18.2 MΩ) for characterization purposes and stored in PBS for cell culture studies.

Scanning electron microscopy (SEM)

SEM was used to characterize the size and morphology of polyelectrolyte shells. A drop of shell sample was placed on a flat mica surface and gently dried under nitrogen gas. A thin film of palladium (Pd, ~2-nm thickness) was sputter-coated to minimize electron charging on the sample surface. A low voltage of 5 kV was used during sample examination on a Hitachi S-4500 scanning electron microscope (Hitachi Ltd., Japan).

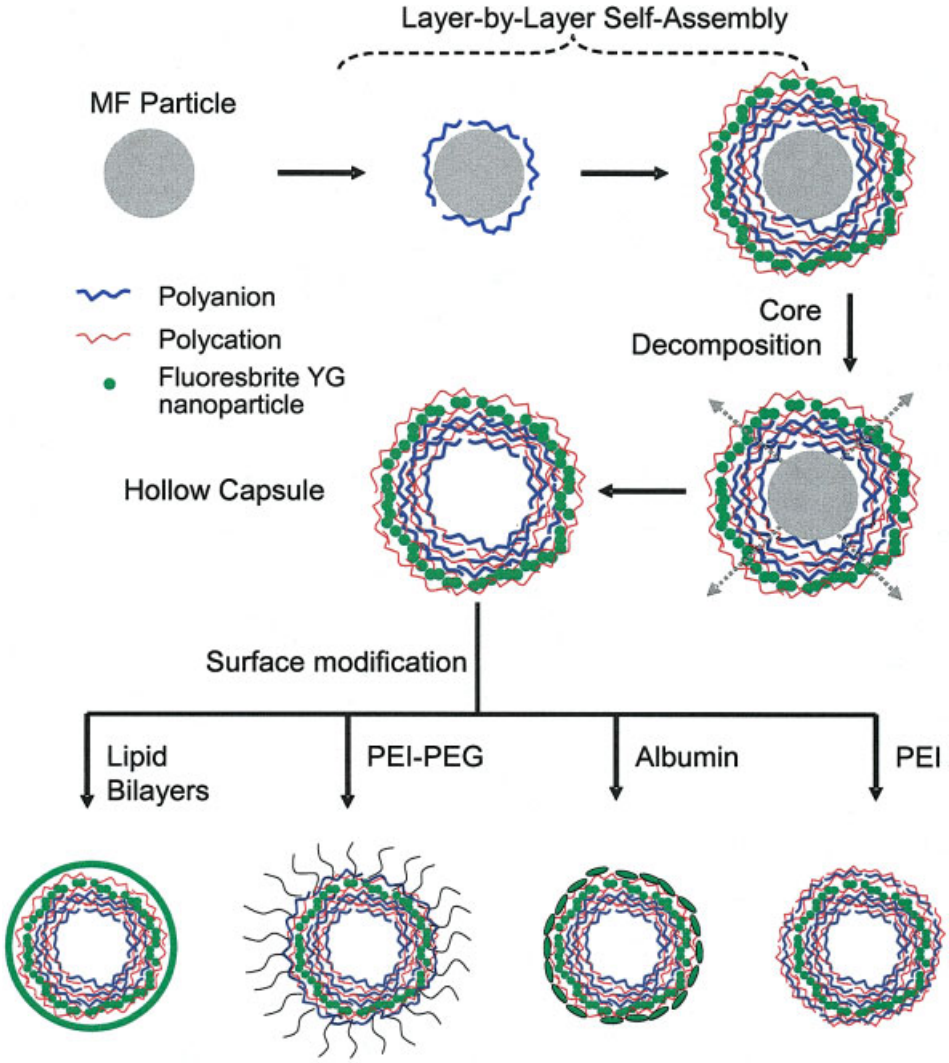

Figure 1. Schematic illustration of productions of hollow polyelectrolyte shells. The common shell structure in this study is [(Gelatin/PDDA)$_5$ + (YG-nanoparticle/PDDA)]. Different polycations (PEI, PLL, PDDA, and PAH) and polyanions (PSS, albumin, and lipid bilayers) were further introduced as the outermost layer to control the shell surface compositions. [Color figure can be viewed in the online issue, which is available at www.interscience.wiley.com.]

Zeta potential measurement

The zeta potential of polyelectrolyte shells with different outermost layers was determined by using a zeta potential analyzer (Zeta Plus, Brookhaven Instruments Corp.). Three samples of each shell formulation were measured at 25°C in a 1 m*M* KCl solution. To investigate how shell surface charge can be altered by serum proteins, polyelectrolyte shells were also incubated in cell culture medium (5% fetal bovine serum) for 1 h and washed with deionized water before measurement.

Cell culture

Human breast cancer MCF-7 cells were obtained from American Type Culture Collection (ATCC, Manassas, VA). Cells were maintained in Roswell Park Memorial Institute (RPMI) media supplemented with 5% heat-inactivated fetal bovine serum, 2 m*M* L-glutamine, 5000 U/mL penicillin and 5 mg/mL streptomycin, and incubated at 37°C in a humidified atmosphere with 5% CO_2. For experimentation, MCF-7 cells were seeded onto six-well plates at a density of 4.0×10^5 cells/well under the aforementioned conditions for 1 day before addition of LbL shells for cell uptake studies.

Flow cytometry

Flow cytometry was used to quantitatively measure the percentage of cells containing internalized shells. Fluoresbrite® YG Carboxylate nanoparticles labeled shells (2×10^7/mL) were suspended in 2 mL of culture medium and added into each well containing MCF-7 cells as indicated above, and incubated for 4 or 24 h. At the indicated time, medium (including the free shells) was removed and cells

were detached using ethylenediaminetetraacetic acid (EDTA) and trypsin. Cell pellets were collected by centrifugation (500*g*, 5 min) and resuspended in PBS. To remove shells attached to the cell surface, cells were washed following a previous protocol (5 m*M* EDTA, pH 5.0 for 15 min).[18] After filtration through a 50-micron nylon mesh, cell suspensions were analyzed using a Beckman Coulter Epics XL-MCL flow cytometer (15 mW argon ion laser). Data analyses were conducted using a WinMDI program (version 2.8).

CLSM

Cells were incubated in shell-containing medium for 4 h before CLSM examination. To identify shell location, cell nuclei and membranes were stained with Hoechst 33342 and lipophilic tracer DiI (Molecular Probes, Inc.), respectively. Samples were examined by CLSM using a Zeiss LSM 510 microscope (Zurich, Switzerland, lasers: He–Ne 543/633 nm, Ar 458/488/514 nm, Ti: Sapphire 700–900 nm) with a confocal plane of 300 nm. Z-sectioning was used for shell morphology investigation, and identification of shell intracellular location. Image processing was performed on an IBM Graphics workstation using Zeiss LSM 510 software.

RESULTS

Characterization of shell morphology by SEM and CLSM

Figure 2(A, B) shows MF particles before and after assembly of five bilayers of gelatin and PDDA, respectively. The original MF particles had a uniform size distribution and their surfaces were smooth [Fig. 2(A)]. After self-assembly of gelatin and PDDA [$(Gelatin/PDDA)_5$], there were no observable changes in particle diameter and spherical shape. However, particle surfaces were slightly rougher and adjacent particles appeared to be bonded through adsorbed polymers [Fig. 2(B), see arrows]. It should be noted that the same particles were well dispersed without observable aggregations in solution under optical microscopy (data not shown). Therefore, it is likely that particle bonding is a result of polymer association at the particle surface during the drying process for SEM sample preparation.

Figure 2(C) shows MF particles coated with an additional bilayer of fluorescent nanoparticles (50 nm) and PDDA [total composition: $(Gelatin/PDDA)_5$ + (YG-nanoparticle/PDDA)]. All the particles maintained an overall spherical shape, however, each particle surface appeared to be grainy. SEM examination of an individual particle under high magnification [Fig. 2(D)] illustrates the adsorption of Fluoresbrite® nanoparticles. The distribution of these nanoparticles (50 nm in diameter) appeared to be dense and uniform on the MF particle surface. Close examination further illustrates that these nanoparticles were not isolated on the MF particle surface, but were bound together by the outermost PDDA layer.

After the above-mentioned polymer layers and nanoparticles were assembled, MF cores were decomposed by acid hydrolysis in a pH 1.2 HCl solution for 2 min. Figure 2(E) shows the SEM image of the resulting polyelectrolyte shells. The shells maintained the same grainy surface morphology as the precursor particles [Fig. 2(C)], suggesting the preservation of fluorescent nanoparticles and associated polymer layers. Meanwhile, shell morphology changed from spherical shape for the precursor particles to that resembling flattened discs [Fig. 2(E)], primarily because of shell collapse during the sample drying process. Consequently, the shell diameters (1.36 ± 0.05 μM) became larger than the precursor particles (0.90 ± 0.01 μM). The shell flattening effect was not observed in solution. Under confocal laser scanning microscope, shells were well dispersed in PBS buffer without observable aggregations [Fig. 2(F)].

Control of surface charge and composition of LbL shells

To control the final surface composition of LbL shells, we used different polycations (PDDA, PEI, PLL, and PAH) or polyanions (PSS, albumin, and lipid bilayers) as the outermost layer for the shells (Fig. 1). Figure 3 shows the zeta potential values for shells with different surface compositions in 1 m*M* KCl solution. Apparently, shells containing a polycation outermost layer had a positive electrostatic potential whereas shells with polyanions possessed a negative potential. Shells with PDDA and PEI outermost layers presented the strongest positive charges at 43.1 ± 6.4 and 46.5 ± 4.1 mV, respectively. PLL and PAH shells showed relatively weaker charge potentials at 20.6 ± 1.4 and 16.9 ± 2.1 mV, respectively. For shells covered with negatively charged materials, those coated with lipid bilayers had the highest negative charge potential at -45.7 ± 7.0 mV. PSS-covered shells had stronger negative potential (-37.2 ± 2.9 mV) than albumin shells (-22.0 ± 2.1 mV).

Characterization of surface properties of LbL shells under serum conditions

Because shell-cell interactions occur in a serum-containing environment, we studied the effect of serum proteins on the surface properties of polyelectrolyte shells. Shells with different outermost layers were incubated in 5% fetal bovine serum in RPMI media for

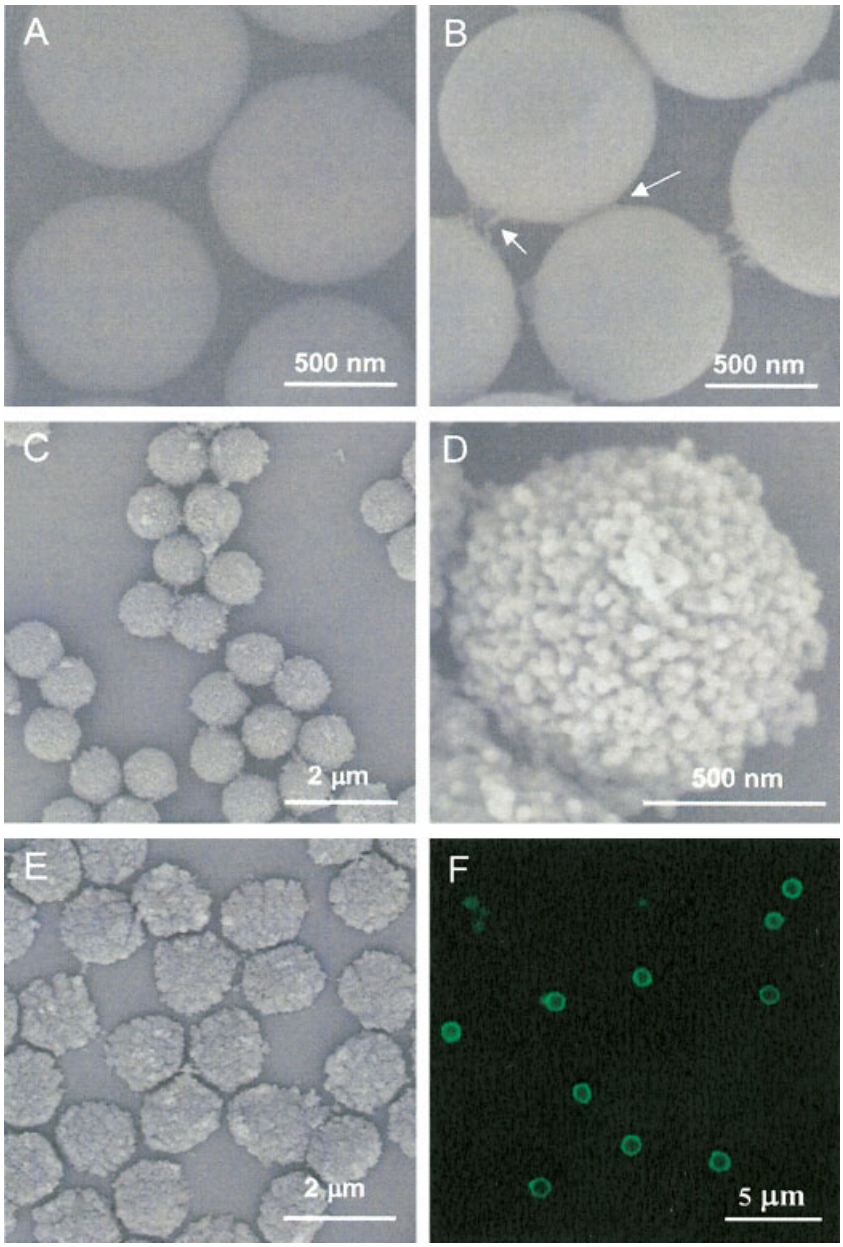

Figure 2. Characterization of polyelectrolyte shells by SEM and CLSM. (A) SEM image of original MF particles without polyelectrolyte coatings. (B) MF particles covered with five bilayers of gelatin and PDDA, $(Gelatin/PDDA)_5$. (C) MF particles covered with $[(Gelatin/PDDA)_5$ + (YG-nanoparticle/PDDA)]. (D) Amplified SEM image of an individual shell in (C). (E) SEM image of hollow shells after MF core decomposition. (F) CLSM image of hollow shells dispersed in PBS buffer. The scale bars are provided in each figure. [Color figure can be viewed in the online issue, which is available at www.interscience.wiley.com.]

1 h. After washing with deionized water, we measured the zeta potential of the resulting shells. The surface electrostatic potential for all polycation-coated shells decreased dramatically (Fig. 3). Except for PEI shells, all other polycation (PDDA, PLL, PAH) shells showed negative electrostatic potentials. More specifically, shells covered with PDDA, PLL, and PAH attained negative potentials at -11.6 ± 2.3, -10.3 ± 3.8, and -13.9 ± 3.1 mV after serum exposure, respectively. Conceivably, adsorption of serum proteins led to the modified shell surfaces and, consequently, the change in zeta potential. The major proteins in the 5% fetal bovine serum RPMI culture medium are bovine albumin, fibrinogen, and globulins that have isoelectric points of 4.9,[19] 5.5,[20] and 5.0–5.1,[21] respectively. They are negatively charged at pH 7.4 and can self-assemble on the positively charged shell surfaces.

For polyanion-coated shells, negative charges were reduced after 1-h incubation in culture media. The zeta potentials were -31.8 ± 3.7, -16.0 ± 7.5, and -14.7 ± 1.2 mV for PSS, lipid, and albumin shells, respectively. The extent of change for polyanion shells

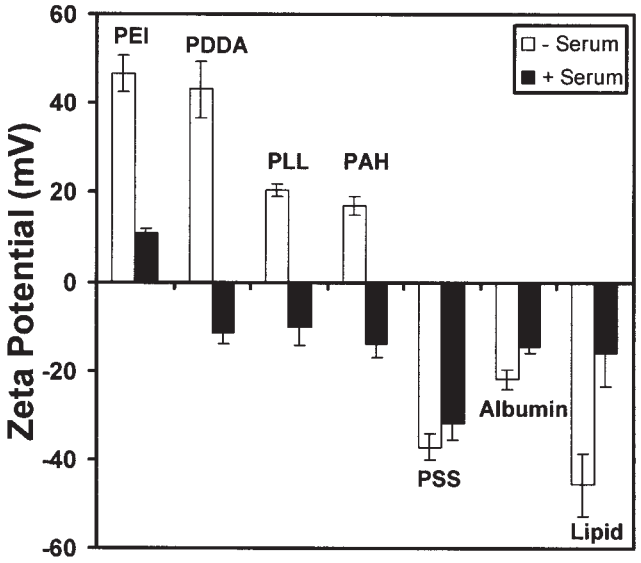

Figure 3. Zeta potential of polyelectrolyte shells with different surface compositions before and after incubations in serum-containing cell culture medium. The error bars were calculated from triplicate sample measurements.

was significantly lower than that for polycation shells. This is consistent with the fact that a majority of serum proteins are negatively charged, which reduces the propensity of protein adsorption to negatively charged polyanion surfaces. For all shells, extended incubation for up to 6 h did not lead to further changes in surface charges, indicating that equilibrium of protein adsorption to the shell surface was reached after 1 h as reported in other studies.[22]

In vitro shell-cell interactions

Given that the fabricated shells contain fluorescent nanoparticles (Ex/Em: 441/486 nm), shell-cell interactions were readily characterized by flow cytometry and CLSM. Figure 4 illustrates representative flow cytometry diagrams for the uptake of PEI shells in MCF-7 cells over time. Each diagram displays two peaks with areas M1 and M2 that correspond to the numbers of cells without or with PEI shell uptake, respectively. The broad M2 peak indicates the heterogeneous population of MCF-7 cells with different number of internalized shells. The ratio of M2/(M1+M2) represents the percentage of cells with internalized shells. For PEI shells, the value of M2/(M1+M2) increased with time within 24 h (Fig. 4) and reached a plateau after 24 h (data not shown). Figure 5 shows uptake of PEI shells by MCF-7 cells after 4-h incubation in shell-containing media. CLSM images showed that multiple PEI shells were internalized into the cell cytoplasm, but not into the nuclei of MCF-7 cells [Fig. 5(C)].

Figure 6 shows the percentage of cell uptake for polyelectrolyte shells with different surface compositions after incubation in serum-containing medium for 4 and 24 h. The highest cell uptake percentage was noted for shells coated with lipid bilayers compared with other groups ($p < 0.01$). Approximately 80% of cells were loaded with shells after 4-h incubation and remained relatively the same after 24 h. Albumin shells exhibited much less cell uptake than lipid bilayer shells, with cell uptake levels of 47 and 49% at 4 and 24 h, respectively. Other groups including PDDA, PAH, PLL, and PSS have shown significant increase of cell uptake from 4 to 24 h. For shells coated with

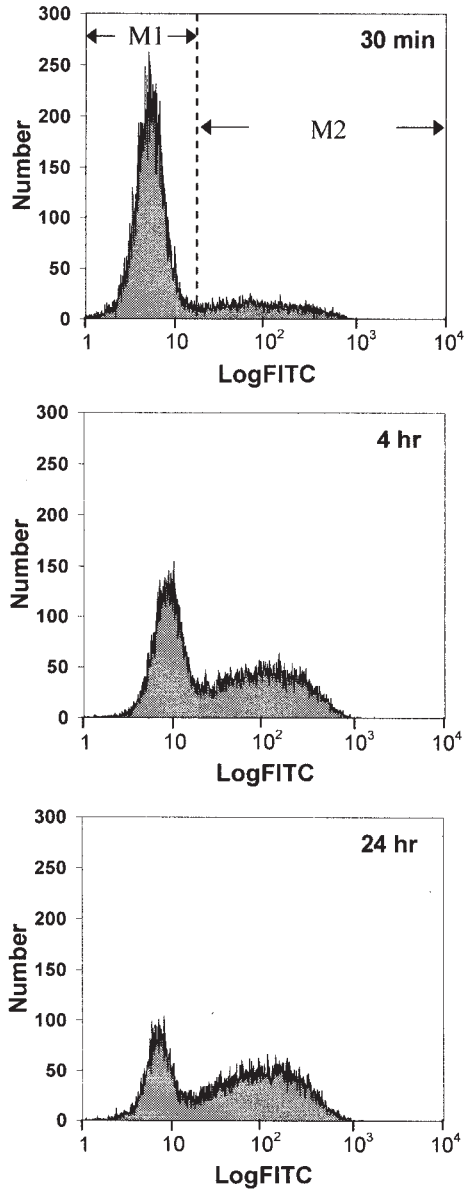

Figure 4. Flow cytometry diagrams of uptake of PEI shells in MCF-7 cells at 0.5, 4, and 24 h. MCF-7 cells were exposed to PEI shells with various outer shell compositions as described in Materials and Methods. M1 and M2 regions represent the populations of cells without and with internalized shells, respectively.

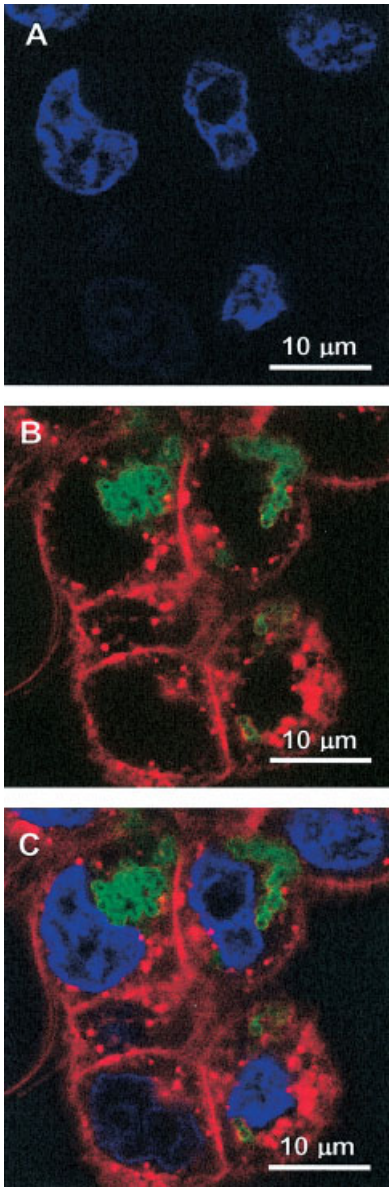

Figure 5. CLSM investigation of shell-cell interactions. (A) MCF-7 cell nuclei (blue) were labeled with Hoechst 33342. (B) Cell membranes (red) were labeled with the lipophilic tracer DiI, and shells (green) were labeled with fluorescent YG-nanoparticles. (C) Overlay images from photomicrographs shown in (A) and (B). The data show that shells were localized in the cell cytoplasm, but not into nuclei of MCF-7 cells. [Color figure can be viewed in the online issue, which is available at www.interscience.wiley.com.]

polycations, PDDA had the highest cell uptake with 70.3 ± 1.6%, whereas PLL shells had the lowest uptake of 47.4 ± 2.7% at 24 h.

Interaction of PEI-PEG shells with MCF-7 cells

Because PEG can effectively reduce protein adsorption on biomaterial surfaces, we studied the cell uptake properties of shells with PEI-PEG surfaces. PEI25k–PEG5k copolymers with three different PEI/PEG graft ratios (PEG1: 1:1; PEG5: 1:5; and PEG10: 1:10) were synthesized and used as the outermost layers for shell assembly. Compared with the electrostatic potential of PEI shells (46.5 ± 4.1 mV), PEI-PEG shells showed a significantly decreased potential ranging from +30 to +32 mV [$p < 0.01$, Fig. 7(A)]. The difference between PEI-PEG shells with different PEG graft ratios was not statistically significant. After shell incubation in serum-containing medium for 1 h, the electrostatic potentials decreased for PEI-PEG shells, but remained above +20 mV for all three PEI-PEG copolymers. Compared with PEI shells, the effect of serum proteins on the decrease of electrostatic potential was much less pronounced for PEI-PEG shells [Fig. 7(A)]. This result was consistent with the shielding property of PEG that can effectively deter protein adsorption.[23]

We used flow cytometry to quantify the percentage of cell uptake for PEI-PEG shells after 4 and 24 h of incubation in serum-containing medium. At 24 h, a higher shell uptake percentage was observed for a lower PEG grafting ratio [Fig. 7(B)]. Shells covered with PEG1 showed highest cell uptake percentage of 68% at 24 h compared with PEI, PEG5, and PEG10 ($p < 0.01$). Increase in PEG graft ratios resulted in a decrease in cell uptake efficiency, strongly demonstrating the stealth effect of PEG chains as reported in other studies.[24] The PEG10 group had the lowest cell uptake compared with all other polycation- and polyanion-covered shells after 24 h of incubation ($p < 0.05$).

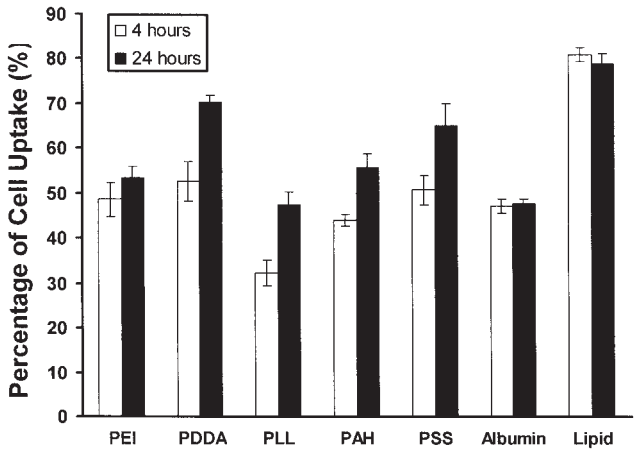

Figure 6. Percentage of cell uptake for shells with different molecular compositions by flow cytometry ($n = 3$). PDDA displays the highest cell uptake percentage of 70.3 ± 1.6% at 24 h among polycation covered shells. Among all groups, lipid bilayers present the highest uptake of 78.7 ± 2.5% at 24 h ($p < 0.05$).

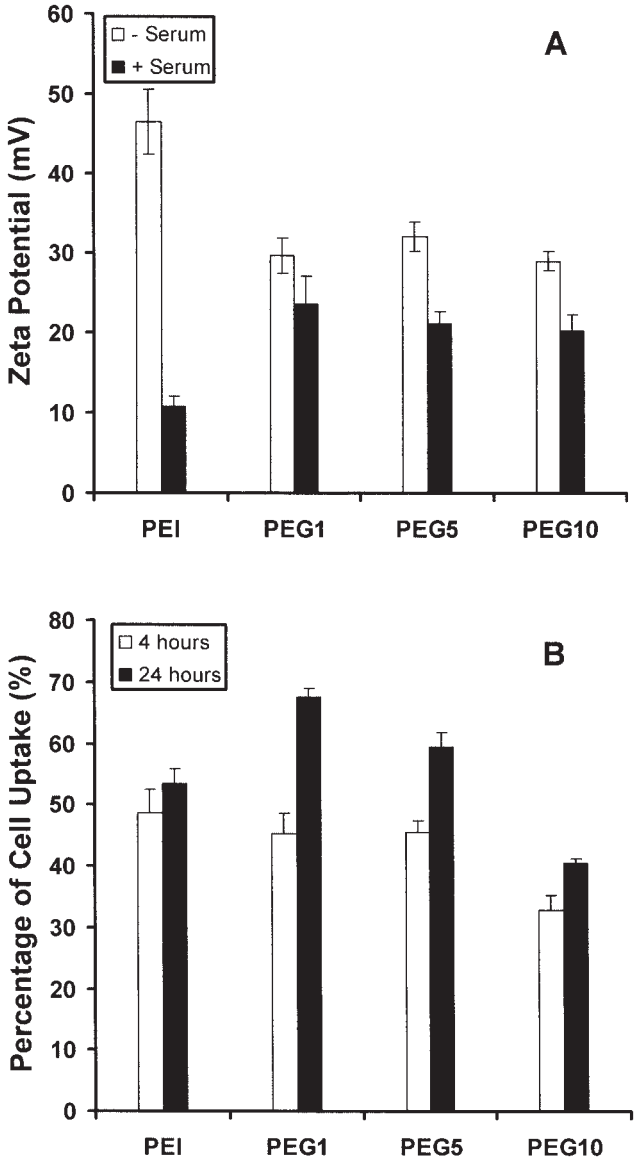

Figure 7. Zeta potential (A) and percentage of cell uptake (B) for polyelectrolyte shells coated with PEI-PEG copolymers. Three PEI/PEG graft ratios were used for the copolymer: PEG1, 1:1; PEG5, 1:5; and PEG10, 1:10. The error bars were calculated from triplicate sample measurements. After 24 h, PEG1 shells allowed the highest percentage of cell uptake ($p < 0.01$) compared with PEI, PEG5, and PEG10 shells.

DISCUSSION

Recently, polyelectrolyte shells have attracted significant attention as a new class of self-assembled structures with potential applications in drug delivery. LbL polyelectrolyte shells were first introduced by the Möhwald group at the Max Planck Institute.[4] Since then, numerous reports have appeared in an effort to understand the physical and chemical properties of shells. LbL polyelectrolyte shells are unique candidates for drug, enzyme, and DNA encapsulation because of the versatile fabrication procedure and easy control of their properties. Small molecular drugs (e.g., doxorubicin)[9] have been successfully encapsulated in polyelectrolyte shells with controllable release kinetics. Enzymes including urease,[8] α-chymotrypsin,[25] and peroxidase[26] have been encapsulated and enzymatic activities were well preserved. Recently, DNA molecules were successfully loaded into shells and its natural double-helix structure was retained.[10] Despite these progresses, reports on the interactions of these shells with biological systems have been scarce. The objective of this study was to investigate polyelectrolyte shells with a variety of surface compositions and study their interactions with cells.

It is widely known that particle surface chemistry has an important role in cell-particle interactions. LbL self-assembly provides a convenient method to control the surface compositions of polyelectrolyte shells. In the proposed study, we produced LbL shells with various surface compositions that provided a wide spectrum of charge properties [e.g., cationic quaternary (PDDA) vs primary (PLL, PAH), secondary and tertiary (PEI) ammonium groups; anionic carboxylates (albumin) vs phosphates (lipid bilayers) vs sulfates (PSS)]. The electrostatic potential varied from $+46.5 \pm 4.1$ (PEI) to -45.7 ± 7.0 mV (lipid bilayers). In the course of this study, we discovered that serum protein adsorption to the shell surface significantly modified the surface composition and charge properties of the original shells (Fig. 3). This was particularly true for cationic shells, because the surface electrostatic potentials were reversed and became negative for PDDA, PLL, and PAH shells after exposure to serum-containing medium. Even for anionic shells, a decrease in surface electrostatic potential was observed although the potential was not reversed. Cell uptake results could not be directly correlated to original surface charge properties because of protein adsorption.

Albumin, globulins, and fibrinogen are three major serum proteins that tend to be adsorbed on colloidal drug carriers.[27] At pH 7.4, serum albumin carries a net negative charge with different charged patches distributed over its surface.[28] As a polyampholyte, it can interact with polycations as well as polyanions.[19] More proteins can be adsorbed on a positively charged surface than a negative one mainly because of the stronger electrostatic interactions. Both albumins and fibrinogen can be adsorbed more onto cationic PAH films than anionic PSS films.[20,28] This is consistent with our findings that surface charge potential changed more dramatically for PAH (16.9 ± 2.1 to -13.9 ± 3.1 mV) than PSS (-37.2 ± 2.9 to -31.8 ± 3.7 mV) shells after serum exposure. The adsorption of proteins on particles leads to changes in surface charges as well as percentage of cell uptake. This was also discovered in other studies because the presence

of albumin on particle surface decreased cell uptake.[14,29]

To reduce protein adsorption on the shell surface, we synthesized PEG-grafted PEI copolymers and incorporated them into the outermost layer of shells. PEG has been used in many drug delivery applications (e.g., stealth liposomes) to prolong the blood circulation times and improve drug pharmacokinetics.[30] In this study, PEI-PEG copolymers have effectively reduced serum protein adsorption as demonstrated by zeta potential measurements. As an example, PEI25k–PEG5k (1:1) shells had less than 15% change in electrostatic potential after serum exposure compared with a 77% reduction for PEI shells [Fig. 7(A)]. Correlation of cell uptake with PEG graft ratios in the copolymers shows that a lower graft ratio (PEG1) led to a much higher percentage of cell uptake than copolymers with lower graft ratios [PEG5 and PEG10, $p < 0.01$, Fig. 7(B)] at 24 h.

In summary, this article describes a comprehensive study of interactions of polyelectrolyte shells with cells *in vitro*. Frequently used LbL self-assembly materials including PEI, PDDA, PAH, and PSS were introduced as outermost layer on shell surface. Confocal microscopy data showed that shells were mostly internalized into the cytoplasm of MCF-7 cells, but not into the cell nuclei. Serum protein adsorption was observed particularly on the surface of polycation-coated shells, suggesting that protein adsorption must be taken into consideration for the biological applications of these shells. PEI-PEG graft copolymers (1:1, 1:5, and 1:10) can effectively reduce protein adsorption on the shell surface. More interestingly, PEI-PEG copolymers with lower grafting density led to higher cell uptake efficiency. These results indicate that choosing an optimal PEG grafting ratio can be beneficial to reduce the degree of serum protein adsorption, and still ensure efficient shell delivery through cell uptake. In conclusion, results from this study provide useful insights on shell-cell interactions and this knowledge will aid the future development of polyelectrolyte shells in drug delivery applications.

The authors thank Dr. Minh Lam for the help on CLSM studies of shells and shell-cell interactions. This research was supported by the NIH R01 CA90696 to J. Gao and NIH R01 CA102792 to D. A. Boothman.

References

1. Ai H, Jones SA, Lvov YM. Biomedical applications of electrostatic layer-by-layer nano-assembly of polymers, enzymes, and nanoparticles. Cell Biochem Biophys 2003;39:23–43.
2. Decher G. Toward layered polymeric multicomposites. Science 1997;227:1232–1237.
3. Lvov Y. Electrostatic layer-by-layer assembly of proteins and polyions. In: Lvov Y, Mohwald H, editors. Protein architecture: interfacial molecular assembly and immobilization biotechnology. New York: Dekker; 2000. p 125–167.
4. Donath E, Sukhorukov GB, Caruso F, Davis SA, Mohwald H. Novel hollow polymer shells by colloid-templated assembly of polyelectrolytes. Angew Chem Int Ed 1998;37:2201–2205.
5. Ibarz G, Dahne L, Donath E, Mohwald H. Controlled permeability of polyelectrolyte capsules via defined annealing. Chem Mater 2002;14:4059–4062.
6. Sukhorukov GB, Antipov AA, Voigt A, Donath E, Mohwald H. pH-controlled macromolecules encapsulation in and release from polyelectrolyte multilayer nanocapsules. Macromol Rapid Commun 2001;22:44–46.
7. Tiourina O, Antipov A, Sukhorukov G, Larionova N, Lvov Y, Möhwald H. Entrapment of chymotrypsin into hollow polyelectrolyte microcapsules. Macromol Biosci 2001;1:209–214.
8. Lvov Y, Antipov AA, Mamedov A, Mohwald H. Urease encapsulation in nanoorganized microshells. Nano Lett 2001;1: 125–128.
9. Ai H, Pink J, Boothman D, Gao J. Layer-by-layer self-assembled nano-organized shells as carriers for doxorubicin. Proceedings of 223rd American Chemical Society National Meeting 2003;226:263-PMSE.
10. Shchukin DG, Patel AA, Sukhorukov GB, Lvov YM. Nanoassembly of biodegradable microcapsules for DNA encasing. J Am Chem Soc 2004;126:3374–3375.
11. Dahne L, Leporatti S, Donath E, Mohwald H. Fabrication of micro reaction cages with tailored properties. J Am Chem Soc 2001;123:5431–5436.
12. McShane MJ, Brown JQ, Guice KB, Lvov YM. Polyelectrolyte microshells as carriers for fluorescent sensors: loading and sensing properties of a ruthenium-based oxygen indicator. J Nanosci Nanotechnol 2002;2:411–416.
13. Foster KA, Yazdanian M, Audus KL. Microparticulate uptake mechanisms of *in vitro* cell culture models of the respiratory epithelium. J Pharm Pharmacol 2001;53:57–66.
14. Thiele L, Diederichs JE, Reszka R, Merkle HP, Walter E. Competitive adsorption of serum proteins at microparticles affects phagocytosis by dendritic cells. Biomaterials 2003;24:1409–1418.
15. Thiele L, Rothen-Rutishauser B, Jilek S, Wunderli-Allenspach H, Merkle HP, Walter E. Evaluation of particle uptake in human blood monocyte-derived cells *in vitro*. Does phagocytosis activity of dendritic cells measure up with macrophages? J Controlled Release 2001;76:59–71.
16. Shuai X, Merdan T, Unger F, Wittmar M, Kissel T. Novel biodegradable ternary copolymers hy-PEI-*g*-PCL-PEG: synthesis, characterization, and potential as efficient nonviral gene delivery vectors. Macromolecules 2003;36:5751–5759.
17. Moya S, Donath E, Sukhorukov GB, Auch M, Balumler H, Lichtenfeld H, Mohwald H. Lipid coating on polyelectrolyte surface modified colloidal particles and polyelectrolyte capsules. Macromolecules 2000;33:4538–4544.
18. Behrens I, Pena AI, Alonso MJ, Kissel T. Comparative uptake studies of bioadhesive and non-bioadhesive nanoparticles in human intestinal cell lines and rats: the effect of mucus on particle adsorption and transport. Pharm Res 2002;19:1185–1193.
19. Houska M, Brynda E. Interactions of proteins with polyelectrolytes at solid/liquid interfaces: sequential adsorption of albumin and heparin. J Colloid Interface Sci 1997;188:243–250.
20. Schwinte P, Voege JC, Picart C, Haikel Y, Schaaf P, Szalontai B. Stabilizing effects of various polyelectrolyte multilayer films on the structure of adsorbed/embedded fibrinogen molecules: an ATR-FTIR study. J Phys Chem B 2001;105:11906–11916.
21. Anfinsen CB, Edsall JT, Richards FM. Advances in protein chemistry. New York: Academic Press; 1985.
22. Lvov Y, Ariga K, Ichinose I, Kunitake K. Assembly of multicomponent protein films by means of electrostatic layer-by-layer adsorption. J Am Chem Soc 1995;117:6117–6123.

23. Prime KL, Whitesides GM. Self-assembled organic monolayers: model systems for studying adsorption of proteins at surfaces. Science 1991;252:1164–1167.
24. Auguste DT, Prud'homme RK, Ahl PL, Meers P, Kohn J. Association of hydrophobically-modified poly(ethylene glycol) with fusogenic liposomes. Biochim Biophys Acta 2003;1616: 184–195.
25. Tiourina OP, Sukhorukov GB. Multilayer alginate/protamine microsized capsules: encapsulation of alpha-chymotrypsin and controlled release study. Int J Pharm 2002;242:155–161.
26. Balabushevich NG, Tiourina OP, Volodkin DV, Larionova NI, Sukhorukov GB. Loading the multilayer dextran sulfate/protamine microsized capsules with peroxidase. Biomacromolecules 2003;4:1191–1197.
27. Luck M, Paulke BR, Schroder W, Blunk T, Muller RH. Analysis of plasma protein adsorption on polymeric nanoparticles with different surface characteristics. J Biomed Mater Res 1998;39: 478–485.
28. Szyk L, Schwinte P, Voegel JC, Schaaf P, Tinland B. Dynamical behavior of human serum albumin adsorbed on or embedded in polyelectrolyte multilayers. J Phys Chem B 2002;106:6049–6055.
29. Moghimi SM, Muir IS, Illum L, Davis SS, Kolb-Bachofen V. Coating particles with a block co-polymer (poloxamine-908) suppresses opsonization but permits the activity of dysopsonins in the serum. Biochim Biophys Acta 1993;1179:157–165.
30. Woodle MC. Controlling liposome blood clearance by surface-grafted polymers. Adv Drug Delivery Rev 1998;32:139–152.